Journal of Alloys and Compounds 509 (2011) 1683–1690

Contents lists available at ScienceDirect

Journal of Alloys and Compounds

journal homepage: www.elsevier.com/locate/jallcom

Corrosion inhibition of 7000 series aluminium alloys with cerium diphenyl phosphate

Julie-Anne Hill[a], Tracey Markley[a,b], Maria Forsyth[a,*], Patrick C. Howlett[a], Bruce R.W. Hinton[a,c]

[a] Department of Materials Engineering and Australian Centre of Excellence for Electromaterials Science, Wellington Rd, Monash University, Clayton, Victoria, Australia
[b] CSIRO, Division of Materials Science and Technology, Clayton, Victoria, Australia
[c] Defence Science and Technology Organisation, Melbourne, Victoria, Australia

ARTICLE INFO

Article history:
Received 29 May 2010
Received in revised form
24 September 2010
Accepted 26 September 2010
Available online 18 November 2010

Keywords:
Aluminium alloys
Corrosion inhibitors
Cerium
Diphenylphosphate
Surface characterisation metals and alloys
Surfaces and interfaces
Scanning electron microscopy
Corrosion

ABSTRACT

Cerium diphenyl phosphate ($Ce(dpp)_3$) has previously been shown to be a strong corrosion inhibitor for aluminium–copper magnesium alloy AA2024-T3 and AA7075 in chloride solutions. Surface characterisation including SEM and ToF-SIMS coupled with electrochemical impedance spectroscopy (EIS) measurements are used to propose a mechanism of corrosion inhibition which appears to involve the formation of a complex oxide film of aluminium and cerium also incorporating the organophosphate component. The formation of a thin complex film consisting of hydrolysis products of the $Ce(dpp)_3$ compound and aluminium oxide is proposed to lead to the observed inhibition. SEM analysis shows that some intermetallics favour the creation of thicker deposits predominantly containing cerium oxide compounds.

1. Introduction

Due to their high strength-to-weight ratio, the wrought aluminium–zinc–magnesium–copper AA7000 series alloys are commonly used in the aerospace industry [1]. The strength of these alloys is developed by the precipitation hardening process. The microstructure of these alloys is heterogeneous and consists of the Al matrix, intermetallic particles (IMPs) and hardening precipitates within the grains, precipitate free zones (PFZ) near the grain boundaries and grain boundary precipitates [2]. Most of the Cu in these alloys is contained in the nanometre size GP (Guinier-Preston) zones and η′ phase. Cu is also present in micrometer size IMPs, which include Al_2CuMg (S phase), Al_2Cu (θ phase) and Al_7CuFe, and the grain boundary precipitate $Mg(ZnCuAl)_2$ (η phase) [2].

The high passivity normally associated with aluminium comes from the highly adherent barrier oxide of Al_2O_3 that forms on the surface. In aqueous environments this protective oxide is formed with a greater thickness and, as long as there is oxygen present, it will continue to repassivate if flaws are formed [3]. However, in the presence of chloride ions (Cl^-), such as in sea water, the oxide is broken down [4] and its repair is hindered [3]. Pitting corrosion in 7000 series alloys has been found to occur near Cu and Fe containing intermetallic particles [2]. Both Cu and Fe are more cathodic than the Al matrix resulting in a galvanic interaction [2]. Meng and Frenkel [2] have studied the corrosion behaviour of a series of 7000 alloys with increasing Cu content all in the T6 temper. They found that in aerated NaCl solutions the polarisation resistance, as determined using EIS, decreased with increasing Cu content, and that the corrosion potential increased with Cu content. Two breakdown potentials were observed during their potentiodynamic polarisation studies [2]. The lower breakdown potential (E_1) was thought to be due to transient dissolution associated with attack of the hardening particles (η′ phase), while the second nobler breakdown potential (E_2) was thought to be due to stable dissolution at the grain boundaries and selective attack within the grains. Meng and Frenkel showed that in a deaerated NaCl solution, these potentials increased with increasing Cu content [2]. It was concluded that the Cu content in the matrix (including the hardening precipitates) controlled this potential [2].

Corrosion protection for these high strength Al alloys is typically provided by chromate conversion coatings or chromic acid anodised coatings with chromate pigmented primer paints. However, due to the toxic and carcinogenic nature of the hexavalent chromate ion [5,6] considerable research has gone into find-

* Corresponding author.
E-mail address: maria.forsyth@deakin.edu.au (M. Forsyth).

0925-8388/$ – see front matter © 2010 Elsevier B.V. All rights reserved.
doi:10.1016/j.jallcom.2010.09.151

ing environmentally friendly alternative protection systems. Salts of the rare-earth metal cerium such as cerium chloride ($CeCl_3$) [4,6–10], cerium nitrate ($Ce(NO_3)_3$) [11–13], cerium sulphate ($Ce(SO_4)_3$) [13], cerium dibutyl phosphate ($Ce(dbp)_3$) [14,15] and cerium diphenyl phosphate ($Ce(dpp)_3$) [16–20] have been investigated for a number of different aluminium alloys.

The inhibition provided by cerium chloride with AA7075 aluminium alloy was thought to occur through the formation of a cerium oxide/hydroxide film [7]. This film was found to initiate at cathodic particles in the alloy where alkaline conditions developed due to the oxygen reduction reaction [7]. The subsequent deposition of cerium oxide/hydroxide film at these sites suppressed this reaction, thereby providing cathodic inhibition [7]. Studies have recently shown that the rare-earth compound cerium diphenyl phosphate $Ce(dpp)_3$ is a strong inhibitor of aluminium–copper–magnesium alloy AA2024-T3 corrosion in chloride solutions [16]. Polarisation studies after 30 min immersion in the test solution have shown that $Ce(dpp)_3$ was a cathodic inhibitor, however after longer immersion times before testing the $Ce(dpp)_3$ was found to be a mixed inhibitor [16].

Recently it has also been shown that $RE(dpp)_3$ compounds (where RE can be Ce, Mischmetal, Praseodymium) also offer excellent corrosion inhibition for the AA7075 alloy [18], which has significantly less Cu content, although detailed characterisation of these surfaces is still required. In this work, we investigate the corrosion inhibition by $Ce(dpp)_3$ for three 7000 series alloys and, in particular, use surface characterisation and electrochemical impedance spectroscopy (EIS) measurements to develop an improved understanding of the mechanism of inhibitor film deposition on these alloys.

2. Materials and methods

2.1. Test specimens and conditions

Specimens 20 mm × 20 mm × 1 mm were used for all tests. They were machined from rolled aluminium alloy plates of AA7022-T651 (25 mm thick), AA7050-T7451 (15 mm thick), and AA7075-T651 (1 mm thick), such that the 20 mm^2 surface was parallel to the rolling direction. The nominal compositions of the alloys used are shown below in Table 1. Prior to testing, specimens were ground to a P4000 finish on 3 M and Norton SiC water-proof abrasive papers under running tap water. All tests were carried out in 0.1 M NaCl, with and without the addition of 150 ppm ($Ce(dpp)_3$) inhibitor using Analar Grade NaCl and distilled water. The initial pH of the test solutions was between 5.5 and 6.0.

2.2. Electrochemical impedance spectroscopy measurements

For all electrochemical measurements, a three electrode flat cell was used with the Al alloy specimen located at one end as the working electrode with an exposed area of 95 mm^2. Electrical connection to the specimen was facilitated through the use of adhesively bonded Cu tape. A high surface area 0.9 mm titanium mesh was used as a counter electrode, and a saturated calomel electrode (SCE) as a reference. The volume of test solution was approximately 300 mL. For tests under aerated conditions, the solution was left open to air before and during tests. The cell assembly was located in a Faraday cage to prevent electrical interference. After immersion the specimen was monitored at the OCP for 5 min, and then the EIS was carried out from 200 kHz to10 mHz with an AC amplitude of 10 mV. After the EIS measurement, the specimen was monitored at the OCP for 24 h after which another EIS experiment was completed. This procedure was repeated 5 times. EC-Lab v. 9.54 software was used to fit equivalent circuits to the impedance data as discussed below. All electrochemical measurements were conducted using a Princeton Applied Research VMP2/z multichannel potentiostat.

2.3. Constant immersion corrosion tests

Specimens were mounted in epoxy resin with the 400 mm^2 surface exposed. They were ground to a P4000 finish on 3 M and Norton SiCwater-proof abrasive papers under running water. The mounted specimens were placed face-up for 6 days in jars containing 85 mL of test solution. The jars were covered with Parafilm™ containing a small hole to provide continuous access of air to the solution. After immersion the specimens were washed with ethanol and distilled water dried, using a nitrogen gas stream, and then placed in a desiccator.

2.4. Surface characterisation

Scanning electron microscopy (SEM) and energy dispersive X-ray spectroscopy (EDS) were carried out on a JSM-6490LA JEOL microscope. Double sided carbon tape was used to cover the edges of the epoxy and form an electrical contact with the aluminium specimens. A 20 kV accelerating voltage was used to image the surfaces and to obtain the energy dispersive X-ray spectra at working distances between 9 and 11 mm.

ToF-SIMS was carried out over an area of 100 μm^2 with a Munster ION-TOF TOF.SIMS IV using a Bi_3^+ ion gun. XPS was carried out with a nominal spot size of 300 $\mu m \times 700$ μm on a Kratos AXIS Ultra DLD machine using monochromated Al Kα radiation. The specimens used were 20 mm × 20 mm × 1 mm and were polished to a 3 μm finish and immersed in 0.1 M NaCl with 150 ppm $Ce(dpp)_3$ for 6 days. They were suspended with fishing line through a 5 mm diameter hole and left open to air.

3. Results

3.1. Constant immersion tests

Optical micrographs of specimens immersed in 0.1 M NaCl with and without the addition of 150 ppm $Ce(dpp)_3$ inhibitor for 6 days are shown below in Fig. 1. For all alloys, there was a clear difference between the specimens immersed in NaCl solution only and those immersed in the NaCl solution with inhibitor. The specimens immersed in the solution containing $Ce(dpp)_3$ had a lighter coloured appearance, and the polishing marks were still visible. There were, however, numerous black spots. Using differential focusing in the optical microscope, these spots were observed to be particles sitting on the surface. Some had a definite crystalline appearance. There was an absence of white corrosion product and no obvious corrosion pits. In comparison, all specimens immersed in NaCl were covered in a layer of corrosion product and pitting was evident. The corrosion product had a characteristic orange-brown colouring possibly associated with the redistribution of Cu from dissolution of the matrix [9]. This coloured effect of the corrosion product was most pronounced with the AA7075 specimen and was not seen on the specimen immersed in solution containing the inhibitor. These observations confirm prior observations from polarisation data, that $Ce(dpp)_3$ is an effective inhibitor for 7000 series alloys [20]. Indeed polarisation data presented in [20] confirm that this inhibitor is a powerful cathodic inhibitor and shifts the corrosion potential to more negative values well below the pitting potential of these alloys. The following additional electrochemical and surface characterisation results are used to build a plausible mechanism for the inhibition process involved here.

3.2. Electrochemical impedance spectroscopy

Impedance and phase angle as a function of frequency for the AA7022-T651 alloy tested in solution with and without the presence of the inhibitor are shown in Fig. 2. These data are typical for all three of the alloys and so only one set of data is presented. These

Table 1
Composition of tested alloys AA7022, AA7075 and AA7050 in wt%.

Alloy	Al	Cr	Cu	Fe	Mg	Mn	Si	Ti	Zn	Zr
AA7022	88.0–92.4	0.1–0.3	0.5–1.0	<0.5	2.6–3.7	0.1–0.4	<0.5	<0.2	4.3–5.2	<0.20
AA7075	87.1–91.4	0.18–0.28	1.2–2.0	<0.5	2.1–2.9	<0.3	<0.4	<0.2	5.1–6.1	
AA7050	87.3–90.3	<0.04	2.0–2.6	<0.15	1.9–2.6	<0.1	<0.12	<0.06	5.7–6.7	0.08–0.15

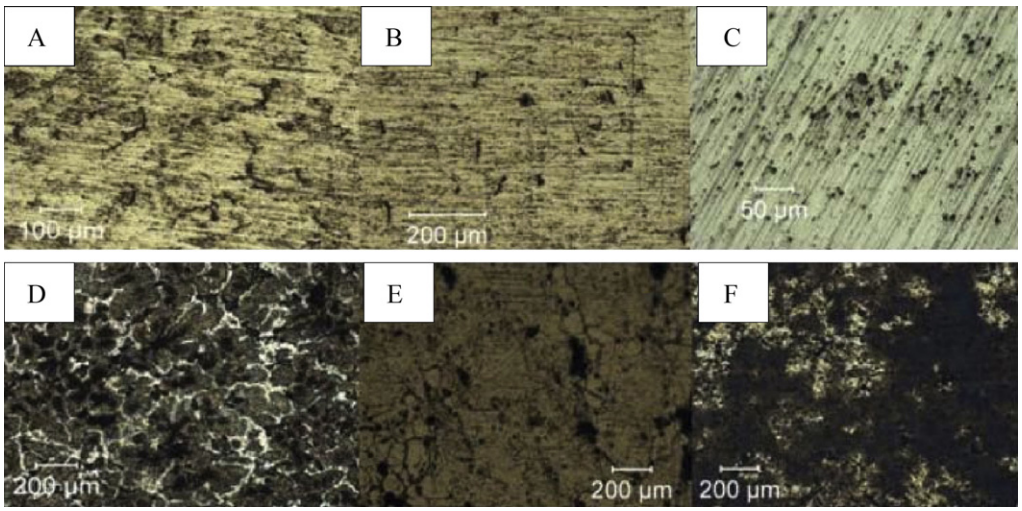

Fig. 1. Specimens exposed to 0.1 M NaCl + 150 ppm $Ce(dpp)_3$: (A) AA7022; (B) AA7050; (C) AA7075 and specimens exposed to 0.1 M NaCl only: (D) AA7022; (E) AA7050; (F) AA7075.

results show that at low frequencies the total impedance was significantly higher when the inhibitor was present after both 5 min and 5 days of testing. The order of magnitude increase in the low frequency impedance plateau indicates significant increase in the resistance to corrosion in the presence of inhibitor. Furthermore, this resistance is present from the initial exposure to inhibitor.

The minima plateau in the phase angle plot (Fig. 2B) for the NaCl after only 5 min immersion shows multiple time constants consistent with active corrosion processes and eventually levels to around −80°. This is close to −90°, which represents the presence of an ideal capacitor [16]. In contrast the presence of inhibitor shows a phase angle more negative than −80° from the initial immersion (after 5 min) and remains relatively unchanged after 5 days (note that the low frequency impedance magnitude also remains constant, consistent with a barrier film). Furthermore the width of these capacitive plateaus when the inhibitor was present was wider than for no inhibitor indicating a capacitive response over a large frequency window and consistent with the presence of a film on the metal surface. The capacitive-like response after 5 days in NaCl solution probably reflects the presence of corrosion products on the metal surface.

Several equivalent circuits that have previously been described to fit EIS data, where one or more superimposed layers are proposed to form on a metal surface [21], were investigated however none of these produced stable fitting across all of the time dependent EIS plots. Instead, the simple Randles circuit consistently provided the best fit to the data although these fits were still not perfect, particularly at the lower frequencies (chi ~ 0.04). Table 2 presents the parameters extracted from the Randles circuits for each of the alloys exposed to either 0.01 M NaCl solution (control specimens) or alternatively a 0.01 M NaCl solution with added $Ce(dpp)_3$ inhibitor (inhibited solutions). The EIS measurements were conducted over a period of 6 days and the fitted parameters for 30 min, 3 days and 6 days are given in the table. In the case of the control specimens, the 7050 alloy containing the most Cu (but least Fe) appears to have the lowest resistance and highest double layer capacitance (previously shown to correlate with a higher level of corrosion [22]) as compared with the 7075 and 7022 alloys. This alloy also seems to show the biggest time dependence for R in the presence of inhibitor, although the value of R after 6 days is not significantly different amongst these alloys. Interestingly the double layer capacity also decreases by a substantial amount in the presence of inhibitor. This observation, combined with the almost 20-fold increase in R in the inhibited solutions and the increased Warburg impedance, supports the fact that $Ce(dpp)_3$ is an excellent inhibitor for the aluminium alloys. The Warburg impedance is usually associated with mass transport limitations and could be interpreted here as being due to the presence of a more resistive film as compared with the

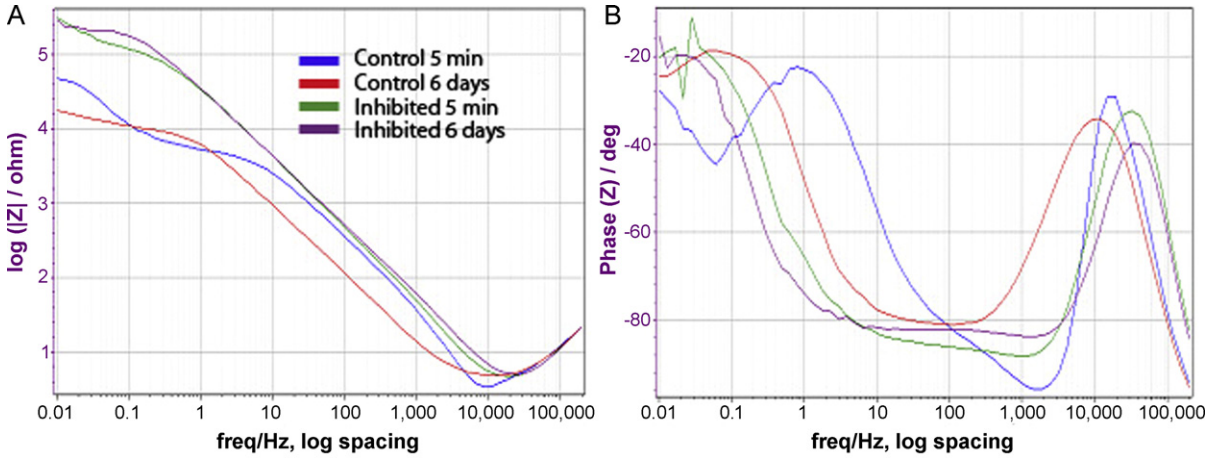

Fig. 2. Bode Impedance plots for AA7022-T651 tested in 0.1 M NaCl with and without inhibitor. (A) Impedance vs. frequency and (B) phase angle vs. frequency.

Table 2
EIS fitting parameter determined from Randles circuit fit to the data. A CPE was used in the equivalent circuit and the alpha parameter was consistently between 0.89 and 0.91. C_{dl} was determined from the CPE using the equation [23] $C_{dl} = (Q_{dl} \times R)^{(1/a)}/R$.

	R, kΩ (7050)	C_{dl}, 10^{-6} F/cm^2 (7050)	W, kΩ s$^{-1/2}$ (7050)	R, kΩ (7075)	C_{dl}, 10^{-6} F/cm^2 (7075)	W, kΩ s$^{-1/2}$ (7075)	R, kΩ (7022)	C_{dl}, 10^{-6} F/cm^2 (7022)	W, kΩ s$^{-1/2}$ (7022)
Control specimens									
30 m	5.3	2.1	5.9	2.8	2.2	6.2	6.2	2.7	2.3
3 d	4.7	2.1	6.6	3.8	2.3	7.2	7.2	3.4	2.1
6 d	6.2	2.8	7.4	3.9	2.3	7.9	7.9	4.2	1.9
Inhibited solutions									
30 m	85	1.5	6.9	122	1.3	17.2	113	0.92	22.2
3 d	133	1.5	5.2	117	1.3	16.6	183	1.04	9.2
6 d	217	1.6	5.7	167	1.4	9.2	198	1.08	26.1

uninhibited cases. The values appear to be greater in the case of AA7075 and AA7022 as compared with the A7050 (nominally the alloy with the highest Cu content). Our initial intention was to correlate the level of inhibition with the Cu content as our prior work on AA2024 suggested that the copper intermetallics were involved in the inhibition process [16–18]; the hypothesis being that the interaction of the inhibitor with Cu containing phases may be primarily responsible for shutting down the cathodic reactions and hence stifling the overall corrosion processes on these alloys. However, the lack of any obvious correlation in the data presented here may indicate that, not only the amount of alloying elements, but also their size and distribution may be important. Unfortunately the heat treatments for the materials obtained in this work were not uniform across the alloys and hence it is hard to draw firm conclusions. Furthermore, even though the Cu contents are lower in the 7075 and 7022 alloys, the Fe content is substantially higher and this may also lead to active secondary phases that may affect the inhibition process.

EIS fitting parameter determined from Randles circuit fit to the data. A CPE was used in the equivalent circuit and the alpha parameter was consistently between 0.89 and 0.91. C_{dl} was determined from the CPE using the equation [23] $C_{dl} = (Q_{dl} \times R)^{(1/a)}/R$.

Finally, the fact that the Randles circuit gave the best fits for the data obtained here could suggest that a number of processes are present with similar time constants, or more likely, that only one process (e.g. diffusion of species through an inhibitor surface film) dominates the electrochemical behaviour of this system.

3.3. Scanning electron microscopy (SEM)

Typical SEM images with EDXS spectra from specimens of the three alloys exposed to 0.1 M NaCl with 150 ppm $Ce(dpp)_3$ for 6 days are shown in Figs. 3–5. The clearly visible polishing marks on the surfaces indicate the absence of widespread corrosion in the presence of the inhibitor. Small particles rich in Ce atoms were observed on all alloys (for example Fig. 3). These particles tended to congregate in small discrete clusters. In some cases, these particles were associated with intermetallic particles (IMPs) in the microstructure (for example particle no. 1 in Fig. 3, and particle no. 1 in Fig. 4). In other cases these particles were distributed over the matrix away from IMPs. It was found that the Ce rich particles were only associated with IMPs that contained Cu or Cu and Fe (for example Fig. 5). An example of such an IMP could be Al_7CuFe. They were not associated with particles that did not contain these elements (for example particle no. 2 in Fig. 4).

Many more Ce rich particles associated with IMPs and distributed over the matrix were observed on AA7050 and AA7075 surfaces than on AA7022. This is consistent with less Cu in the AA7022 alloy and thus presumably fewer IMPs. Furthermore the number of Ce counts in the EDXS spectra was generally higher for the particles found on AA7050 and AA7075 than for AA7022. The dramatic protection of the surface against corrosion in 0.1 M NaCl with inhibitor present would suggest that the inhibitor coverage is likely to be over the entire surface however the EDXS measurement is not surface sensitive, having a relatively large interaction volume. Markley et al. [16] have suggested that on AA2024 alloy immersed in a $Ce(dpp)_3$ containing NaCl solution, Ce could not be detected in the protective film that formed because that film was too thin. The observation of a more distinctly capacitive behaviour of the EIS data for the inhibited systems also suggests the presence of a thin film.

High resolution SEM was also used to examine the surface of polished AA7075-T6 specimens before and after exposure to $Ce(dpp)_3$ solutions to confirm the presence of a protective film on the surface

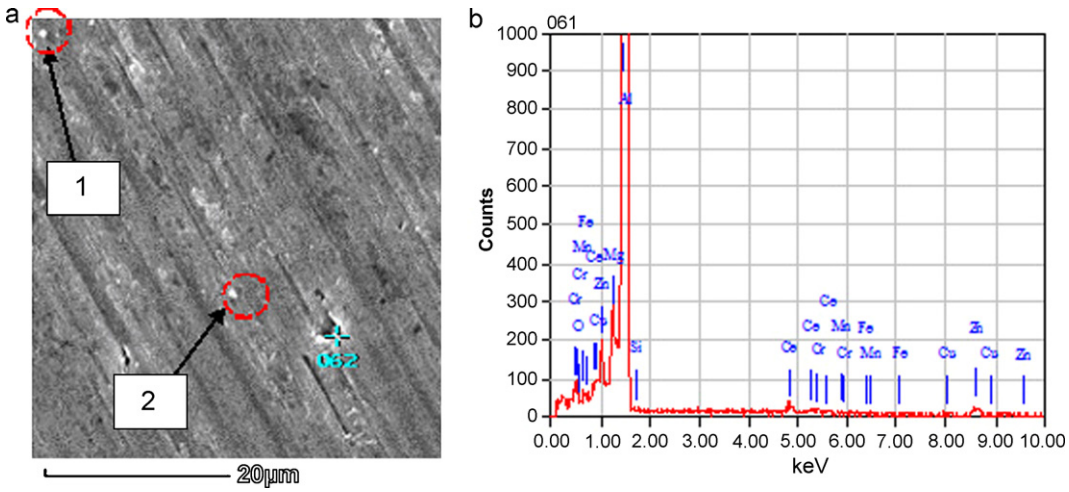

Fig. 3. (A) SEM photograph and (B) corresponding EDS scan of particles 1 and 2 on inhibited AA7022-T651 aluminium alloy.

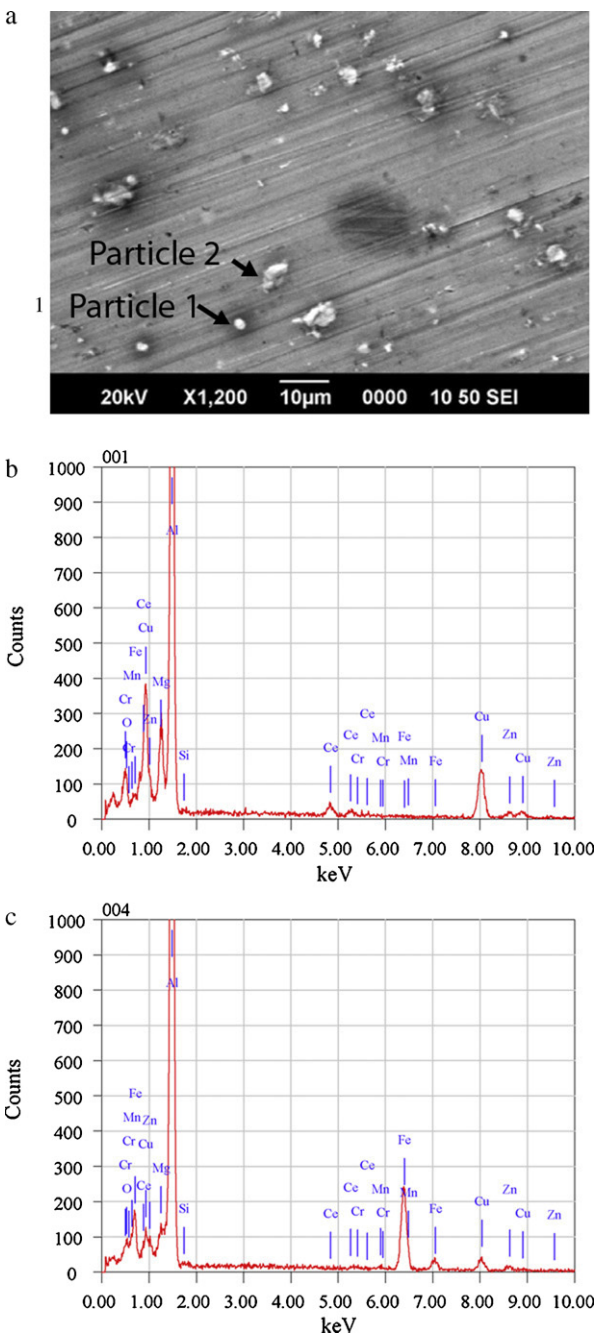

Fig. 4. (A) SEM photograph and corresponding EDS scans of (B) particle 1 and (C) particle 2 on inhibited AA7075-T6 aluminium alloy.

of the inhibited specimens (Fig. 6). SEM micrographs of the polished AA7075-T6 surface before exposure to any test solutions are shown at two magnifications, and highlight the prominent polishing scratches on an otherwise featureless surface. After the polished AA7075-T6 specimen had been exposed to an uninhibited 0.1 M NaCl solution for 7 days, SEM and EDXS showed the alloy surface to be extensively covered with two discrete layers of corrosion product. In the inset to Fig. 6C, the underlying matrix can be seen through a cracked layer that EDXS (not shown) showed to be aluminium oxide with some sodium present, and a sparse top layer also consisting of aluminium and oxygen.

Fig. 6C and D shows the result of exposure of a polished AA7075-T6 specimen to a 0.1 M NaCl solution containing 200 ppm $Ce(dpp)_3$ for 7 days before SEM imaging. The lower magnification images still showed the polishing marks, however at the higher magnification shown here, the roughness of the surface was quite evident, and indeed suggests the presence of a film covering the entire surface. The film is, however, likely to be quite thin given that at lower magnifications the image was similar to the as polished alloy surface.

Fig. 7 compares the scanning electron micrographs of microtomed AA7050 aluminium alloy surfaces after immersion in NaCl solution with and without the $Ce(dpp)_3$ inhibitor. These show the clear differences between the surfaces when the inhibitor is present even at such low concentrations. On the specimen immersed in NaCl solution only a typical mud-cracked pattern was observed in the thick corrosion product. On the surface of the specimen immersed in solution with the inhibitor, polishing marks are still clearly visible indicating that the film is very thin. Moreover, it appears that the coverage of this film was extensive over the surface.

3.4. Time-of-flight-secondary-ion-mass-spectroscopy (ToF-SIMS)

Selected negative and positive maps from an analysis of the spectra for a specimen of AA7050 exposed to NaCl solution with the inhibitor for 6 days are shown in Figs. 8 and 9. The negative maps indicate the widespread presence of both P and Al oxides over the entire surface area (100 μm^2) sampled. The total ion count is low, again suggesting that any film present is thin. The dominant features of the positive maps are the widespread coverage of Ce oxides and hydroxides with some very high local concentrations. These localized concentrations are consistent with the clusters of Ce rich particles observed with SEM and EDS. Furthermore, the ToF-SIMS provides direct evidence of the phosphate moieties as well as organic fragments such as C_6H_6O and C_3H_7/C_2H_5 which are evidence for the presence of the organophosphate component of the $Ce(dpp)_3$ inhibitor. The presence of aluminium oxides, phosphorous oxides and cerium oxides suggests that the inhibiting layer is indeed a complex combination of the rare earth inhibitor and aluminium oxides as discussed further below.

4. Discussion

4.1. Nature of the protective film

The inhibition observed is likely due to the formation of a complex protective film on the surface of the alloy, as evidenced by various surface analysis techniques discussed here. The film consists of discrete particles rich in Ce and clearly visible in both the optical microscope, SEM and ToF SIMS. The ToF SIMS evidence indicates that these particles were predominantly Ce oxide/hydroxide. They were present on top of, or possibly emergent from, a background film which covered the entire surface. This background film was very protective as shown by the retention of polishing marks and the absence of any corrosion product. The ToF SIMS data indicate that this film was very thin and consisted of P, Al and Ce oxides. The presence of both Ce and P together suggests that the $Ce(dpp)_3$ may be largely intact on the surface. Raman spectroscopy results by Markley et al. [18] with AA2024 and $Ce(dpp)_3$ also suggested that the $Ce(dpp)_3$ was present intact on the surface of that alloy.

The results from the EIS scans also support the formation of a continuous and protective film over the aluminium surface.

4.2. Formation of the protective film

Over recent years, several possible mechanisms for corrosion inhibition by these rare earth organic inhibitor compounds have been discussed. Markley [18] has suggested that, for an AA2024 alloy exposed to the $Ce(dpp)_3$ inhibitor, the protective film consists of Al oxide and a deposited film of $Ce(dpp)_3$. The inhibitor initially

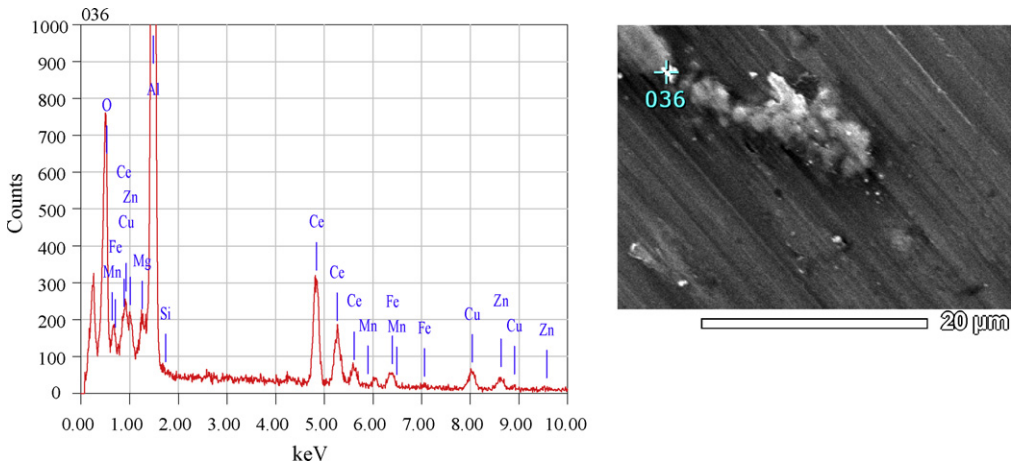

Fig. 5. SEM photograph of inhibited AA7050-T7451 alloy surface and corresponding EDS spectra of particles.

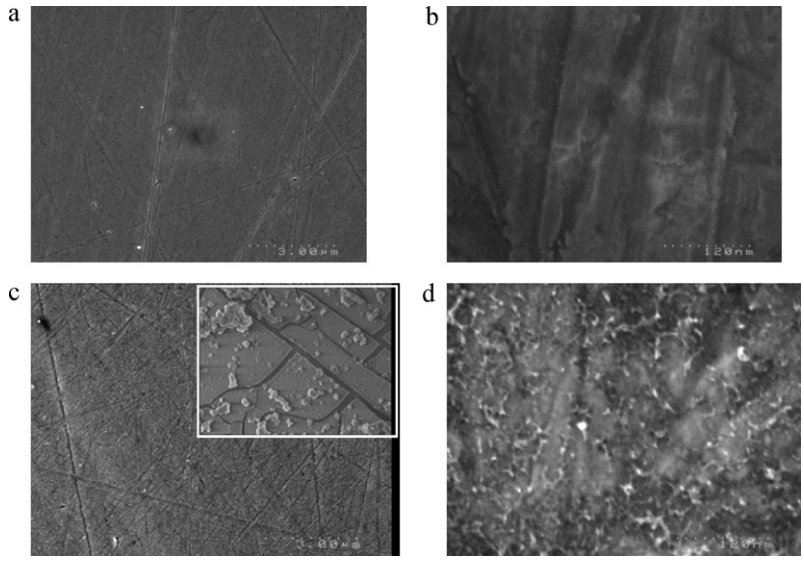

Fig. 6. Secondary scanning electron micrographs of polished AA7075-T6 (A) before exposure 5k× magnification and (B) 125k× magnification (C) after exposure to 0.1 M NaCl and 200 ppm Ce(dpp)$_3$ 10k× magnification and (D) after exposure to 0.1 M NaCl and 200 ppm Ce(dpp)$_3$ at 250× magnification. The inset in Fig. 5(C) shows the surface of the alloy after immersion in 0.1 M NaCl solution with no inhibitor present. The inset in (C) shows mud-cracking and clouds of aluminium corrosion product on the alloy surface. The polishing marks visible before immersion cannot be seen due to the level of corrosion, whereas in (C) the surface looks almost identical to (A), where the aluminium has not been immersed.

deposits at electrochemically active sites such as cathodic intermetallic particles, and on the bulk matrix as a thin surface film. This film is supplemented by a further Al oxide layer on the surrounding matrix, thereby accounting for the strong AlO signal observed in the ToF SIMS experiments shown above. For studies with steel and Ce carboxylate inhibitors, Deacon et al. have suggested that those inhibiting compounds may interact with the steel to form bimetallic complexes of Fe and Ce [24,25]. It is possible that a similar mechanism applies in the case of Ce(dpp)$_3$ [19]. Markley has shown that the Ce(dpp)$_3$ may remain in solution as a complex rather than separate into the individual Ce^{3+} and dpp^- components. Near the surface, partial hydrolysis of the Ce organic bonds can occur driven

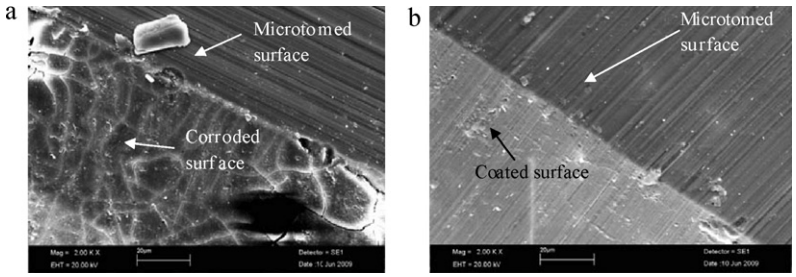

Fig. 7. Scanning electron micrographs of microtomed surface showing (A) a corroded specimen of AA7050 after immersion in 0.1 M NaCl and (B) a protected specimen of AA7050 after immersion in 0.1 M NaCl with 150 ppm Ce(dpp)$_3$. The sharp interface running diagonally separates the fresh metal surface from the post immersion surface for a pyramidal specimen. The 'mud-cracking' pattern in (A) is indicative of corrosion product on aluminium metal and alloys.

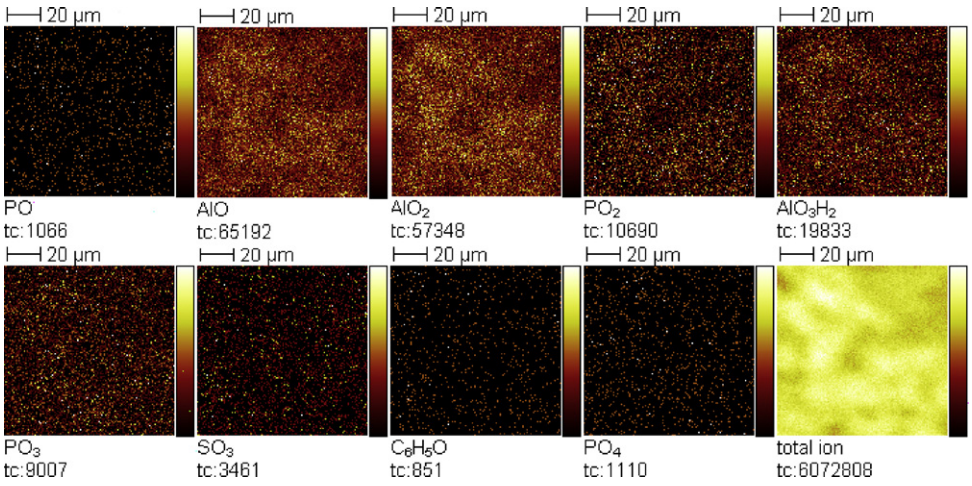

Fig. 8. Negative ToF-SIMS maps for AA7050-T7451after 24 h immersion in an inhibited aqueous chloride solution.

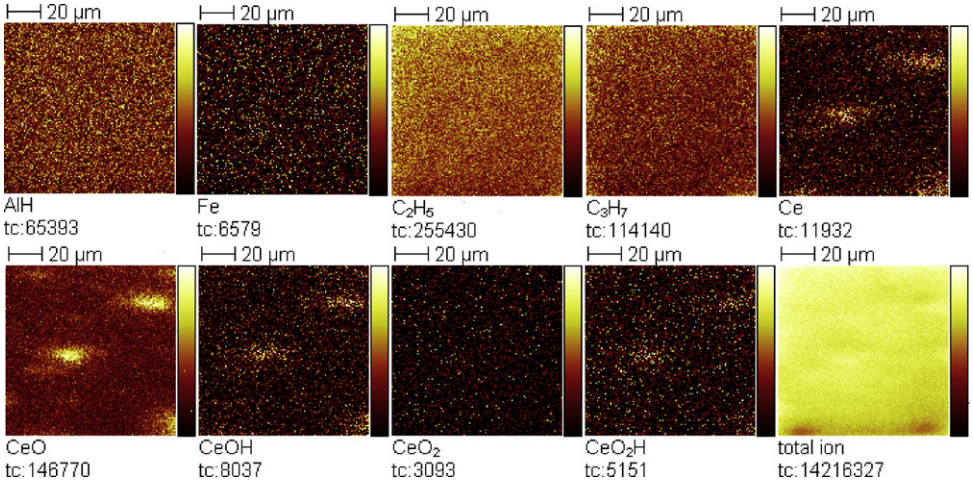

Fig. 9. Positive ToF-SIMS maps for AA7050-T7451 after 24 h immersion in an inhibited aqueous chloride solution.

by the local pH increases resulting from the reduction of oxygen occurring locally at cathodic sites. The free Ce bonds on the inhibitor complex are then able to coordinate with Al surface atoms to form an Al/Ce bimetallic complex compound which constitutes the protective, insoluble film. Localized regions of high pH may lead to complete hydrolysis of all the Ce organic bonds. As a result the precipitation of discrete Ce oxide/hydroxide particles occurs when the solubility product of the Ce oxide/hydroxide is reached. In addition, Al ions in solution may react with free organophosphate to precipitate an insoluble Al phosphate film. Thus the protective film is likely to have a very complex composition as shown by the ToF SIMS results. A corrosion event is required to produce the OH^- ions and Al ions involved in the mechanism described above. This event is clearly minor as no large scale evidence of corrosion was detected. One possibility is the de-alloying of the hardening precipitates $Mg(ZnCuAl)_2$ driven by the presence of Cu.

Unlike the natural alumina film which breaks down in the presence of Cl^- ions, the film formed by the inhibitor maintains its integrity after extended exposure. This film was considerably more resistive than that measured from the control for these 7000 series alloys.

5. Conclusions

The rare-earth inhibitor $Ce(dpp)_3$ has been shown to be an effective inhibitor on AA7022, AA7075 and AA7050 aluminium alloys in a chloride environment, significantly decreasing the corrosion rates of all alloys. SEM analysis of the specimens showed a fine distribution of discrete Ce containing particles on the alloy surface, either on the matrix or over cathodic Cu containing intermetallics. The uncorroded surfaces of the specimens immersed in 0.1 M NaCl + $Ce(dpp)_3$ suggest the presence of a film over the entire surface, ToF-SIMS data indicated that a complex Ce/Al organophosphate film was present although this was not necessarily homogeneous over the surface.

Acknowledgements

The authors would like to thank the Defence Science and Technology Organisation for assisting with and allowing use of their SEM and optical microscope facilities and Robert Jones at LaTrobe University for use of ToF-SIMS equipment. JH gratefully acknowledges The Australian Centre of Excellence for Electromaterials Science for a vacation research scholarship.

References

[1] R.E. Smallman, R.J. Bishop, Modern Physical Metallurgy and Materials Engineering, Elsevier Butterworth-Heinemann, 1999.
[2] Q. Meng, G.S. Frenkel, Journal of the Electrochemical Society 151 (2004) B271–B283.
[3] M. Schumacher, Seawater Corrosion Handbook, William Andrew Publishing/Noyes, 1979.
[4] M. Dabala, E. Ramous, M. Magrini, Materials and Corrosion 55 (2004) 381–386.
[5] T. Wang, Y.J. Tan, Materials Science and Engineering B 132 (2006) 48–53.

[6] B.R.W. Hinton, Journal of Alloys and Compounds 180 (1992) 15–25.
[7] D.R. Arnott, B.R. Hinton, N.E. Ryan, Materials Performance 26 (1987) 42–47.
[8] A.K. Mishra, R. Balasubramaniam, Materials Chemistry and Physics 103 (2007) 385–393.
[9] M. Kabasakaloglu, H. Aydin, M.L. Aksu, Materials and Corrosion 48 (1997) 744–754.
[10] A.E. Hughes, R.J. Taylor, B.R.W. Hinton, L. Wilson, Surface and Interface Analysis 23 (1995) 540–550.
[11] M. Bethencourt, F.J. Botana, M.J. Cano, M. Marcos, Applied Surface Science 238 (2004) 278–281.
[12] K.A. Yasakau, M.L. Zheludkevich, S.V. Lamaka, M.G.S. Ferreira, Journal of Physical Chemistry B 110 (2006) 5515–5528.
[13] A. Decroly, J.-P. Petitjean, Surface & Coatings Technology 194 (2005) 1–9.
[14] N. Birbilis, R.G. Buchheit, D.L. Ho, M. Forsyth, Electrochemical and Solid-State Letters 8 (2005) C180–C183.
[15] D. Ho, N. Brack, J. Scully, B.R.W. Hinton, M. Forsyth, Journal of the Electrochemical Society 153 (2006) B392–B401.
[16] T.A. Markley, M. Forsyth, A.E. Hughes, Proceedings ACA Corrosion and Prevention 2007, 2007.
[17] T.A. Markley, E. Anthony, Hughes, C. Teck, Ang, Electrochemical and Solid-State Letters 10 (2007) C72–C75.
[18] (a) T.A. Markley, M. Forsyth, A.E. Hughes, Electrochimica Acta 52 (2007) 4024–4031;
(b) T.A. Markley, Ph.D. Dissertation, Monash University, Australia, 2008.
[19] M. Forsyth, T. Markley, D. Ho, G.B. Deacon, P. Junk, B. Hinton, A.E. Hughes, Corrosion 64 (2008) 191–197.
[20] J.-A. Hill, T. Markley, M. Forsyth, P. Howlett, B. Hinton, Proceedings ACA Corrosion and Prevention 2008, 2008.
[21] (a) R. Baboian, Corrosion Tests and Standards: Application and Interpretation, 2nd ed., ASTM International, 2005;
(b) M.E. Orazem, B. Tribollet, Electrochemical Impedance Spectroscopy, John Wiley & Sons Inc., Hoboken, 2008.
[22] F. Gui, R.G. Kelly, Electrochimica Acta 51 (1997) 2008.
[23] http://www.consultrsr.com/resources/eis/cpecalc.htm.
[24] M. Forsyth, K. Wilson, T. Behrsing, C. Forsyth, G.B. Deacon, A. Phanasgoakar, Corrosion 58 (2002) 953–960.
[25] G.B. Deacon, C.M. Forsyth, T. Behrsing, K. Konstas, M. Forsyth, Chemical Communications 23 (2002) 2820–2821.